FE MODELLING TO SIMULATE THE AXIAL CRUSHING BEHAVIOR OF CFRP COMPOSITES

Kei Saito[1], Masato Nishi[1]

[1] Engineering Technology Division, JSOL Corporation, 2-5-24 Harumi, Chuo-ku, Tokyo, Japan, saito.kei@jsol.co.jp and nishi.masato@jsol.co.jp

Keywords: FEA, Composite Tube, Axial Crushing, Failure, Debris Wedge

ABSTRACT

Axial crushing simulation of a CFRP tube is performed with an explicit finite element solver, LS-DYNA. A physical based material model which considers the realistic damage progression and the failure mechanism of composites is applied to each ply layer. A cohesive zone model is also applied between each layer in order to reproduce interlaminar fractures. The numerical analysis is conducted with several modelling methods, examining the deformation mode and the reaction force. The result shows that the behaviour in the crush front area strongly depends on the modelling method and affects the evaluation point of the structure. It also implies that the prediction of debris wedge formation is a key factor for accurate evaluation in general purpose crushing analysis.

1 INTRODUCTION

Crash simulation of car body structures is especially important in automotive design because of the strict regulations that must be met on the performance of the passive safety of cars. Therefore, characteristics such as failure mode, load response, and energy absorption during the axial crush deformation of a composite structure are of great interest for its crashworthiness assessment. Axial crush behaviour of a composite structure is the consequence of the complex damage progression of each constituent, such as fibre fracture and kinking, matrix cracking and delamination [1, 2]. These damages cause microscopic separation in the material and elasticity is lost due to a decrease in the effective area which can bring stresses. In practical use of numerical simulation, it is quite difficult to model these small scale discontinuities because of numerical issues such as the needs of complex numerical technique and computational cost, and numerical instability. One practical simulation strategy for small scale damages is modelling based on continuum damage mechanics (CDM) [3]. By this method, damage accumulation is considered in a representative unit element, which can be treated as a part of a continuum body. Therefore, CDM is familiar to conventional finite element algorithms and easily implemented in constitutive models. Actually, many existing FE modelling of composite structures are based on CDM for intra-lamina material [4].

However, the capability of these models is still limited due to the complex behaviour of CFRP after damage initiation. Since conventional material models require non-physical and code-specific parameters in order to reproduce the failure characteristics of composites [5], and these parameters significantly affect the crushing response, it is quite difficult to utilize these kinds of material models for arbitrarily designed composite products. Crush behaviour of composites also causes material discontinuities and generates a lot of broken pieces of material due to severe deformation. From the experimental study [1, 2] it has been observed that the debris induces successive material damaging and failure. Therefore, it is important for crush simulation of composite structures to take into account not only material failure but also the effect of the debris from the composites. On the other hand for crash analysis with commercial finite element solvers, it is still common to delete largely deformed and distorted elements during calculation. Although these artificial processes are mandatory for robust simulations, they often cause non-physical energy dissipation and sharp peaks and valleys in the load response of the axial crushing process due to the deletion of elements, i.e. the load reaches the peak at the moment that the active row of elements fail, then it drops to zero [5]. Deleting elements also prevents formation of a debris wedge which should be modelled because it is directly related to the process of damaging, failure, and deformation of plies. To this end, the method of a pre-defined debris

wedge which is artificially placed in the FE model has been applied in order to evaluate the reaction force accurately during progressive failure [6, 7]. Furthermore, it has been reported that detailed models which have high discretization accuracy with a physically based damage model can predict the test results in arbitrarily shaped structures without numerical calibration for post damage initiation behaviour [8]. Since physically damaged elements work like the debris and contribute to the deformation in crush front area, the reaction force and the deformation mode can be reproduced without even an artificial debris wedge. Considering the results of these studies, it is necessary to look into what the effect of element deletion is and what the best modelling is to reproduce the actual behaviour in crush front area, retaining robust simulation even in the severe deformation.

In this paper, the axial crushing simulation of a CFRP tube is performed with an explicit finite element solver, LS-DYNA. Recently, physically based material models and failure criteria [9-12], which do not need calibration against experimental tests, have been implemented and utilized in the solver. In this model, strain softening, which is important to model the damage progression in composites, is regularized using a characteristic element length and its fracture toughness in order to ease the mesh dependency of the damaging process. The simulation model and material properties are chosen from the literature [8, 13]. A way of deleting distorted elements during the evolution of damage and failure is investigated in order to reduce the numerical oscillation in the load response. Furthermore, several FE models with different degrees of element discretization and different debris model sizes are used to identify how they affect the result of the crushing simulation. The result shows that a smoother and more realistic load response is achieved by controlling the deletion of damaged elements. In the study of discretization accuracy, we can see elements which have damage and failure working like the debris wedge, whose size depends on mesh size. The study of the pre-defined debris model shows that the size of the debris wedge strongly affects the deformation mode and reaction force. Finally, the need for further improvement of the numerical modelling to predict the behaviour of the steady crushing process is discussed.

2 FAILURE MECHANISMS OF COMPOSITE TUBE

Typical composite failure modes are shown in Figure 1. Macroscopic behaviour and failure mode of composite structures under compression loading is determined by the combination of these kinds of microscopic failure modes. For better energy absorption of composite structures under compression loading, progressive crushing failure in which a stable micromechanical damage and failure propagates down is generally preferred. In this failure mode, broken and compressed pieces of material, which are the result of material kinking, buckling and cracking, form a debris wedge, which induces micromechanical fracture. Figure 2 shows schematics of the main failure mechanisms of the failure mode, referring to the literature [1, 2, 6] in which the failure process is well described. The debris generated during the crushing event plays an important role to whole deformation mode of the structure. Therefore, reproducing the effects caused by the debris wedge is important for numerical simulations.

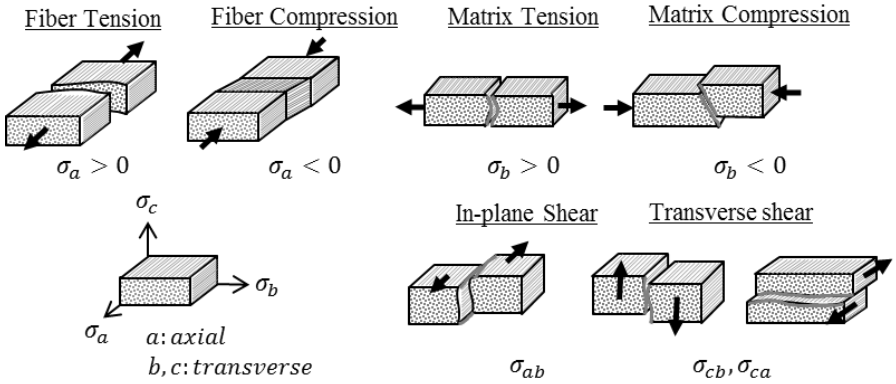

Figure 1: Microscopic failure mode of unidirectional reinforced composite.

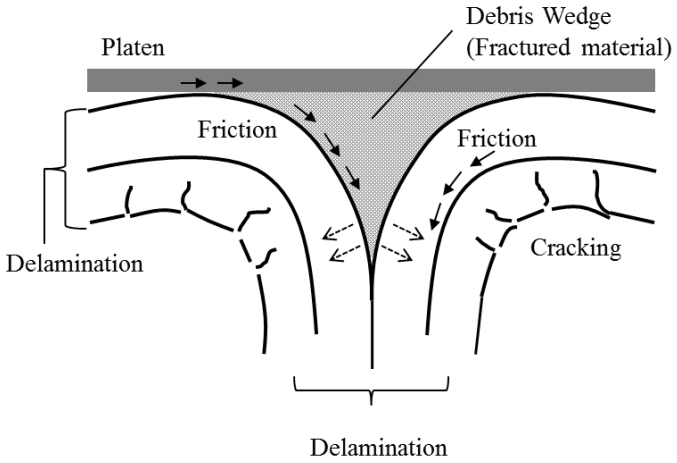

Figure 2: Formation of debris wedge under compression loading.

3 DESCRIPTION OF MATERIAL MODEL

In this section, we briefly describe the material model used in this study. During axial crush deformation of composites, complex failure phenomena such as fibre breakage, fibre kinking, and matrix cracking are observed. To consider the effects caused by these failure mechanisms, non-physical parameters which can adjust the behaviour of the composite structures after damage initiation have been used so that the result can be compared to that from the experiments. However, physical and quantitative parameters which describe damage progression are mandatory in order to improve the accuracy of the simulation in design space.

Recently the damage model introduced by Maimi et.al.[11, 12] was implemented as MAT_262 of the explicit finite element code, LS-DYNA [14]. This material model is basically orthotropic elastic but has a physical damage model based on CDM, which takes fracture toughness as the damage driving parameter. Nonlinear stress-strain relation in in-plane shear deformation is also considered in the model. Furthermore, mesh size dependence of energy dissipation is eased by a regularization technique with characteristic element length. Therefore, the model makes it possible to input the fracture and damage characteristics obtained from experiments directly without any numerical calibration.

3.1 Intra-lamina damage model

The constitutive law is based on the complementary free energy density G. The compliance tensor H is calculated by taking second derivative of G with respect to the stress tensor.

$$H = \frac{\partial^2 G}{\partial \sigma^2} = \begin{bmatrix} \frac{1}{(1-d_1)E_1} & -\frac{\nu_{21}}{E_2} & 0 \\ -\frac{\nu_{12}}{E_1} & \frac{1}{(1-d_2)E_2} & 0 \\ 0 & 0 & \frac{1}{(1-d_6)G_{12}} \end{bmatrix} \tag{1}$$

where $E_1, E_2, \nu_{12}, \nu_{21}, G_{12}$ are the in-plane orthotropic elastic properties. The parameters $d_1, d_2,$ and d_6 represents the damage in fibre direction, transverse direction, and the damage of shear mode. To account for the transverse crack closure under load reversal, these damage variables are defined as

$$\mathrm{d}_1 = d_{1+}\frac{\langle \sigma_{11} \rangle}{|\sigma_{11}|} + d_{1-}\frac{\langle -\sigma_{11} \rangle}{|\sigma_{11}|} \tag{2}$$

$$\mathrm{d}_2 = d_{2+}\frac{\langle \sigma_{22} \rangle}{|\sigma_{22}|} + d_{1-}\frac{\langle -\sigma_{22} \rangle}{|\sigma_{22}|}$$

where $\langle x \rangle$ is the McCauley operator defined as $\langle x \rangle := (x + |x|)/2$.

The failure surface in which the material exhibits elastic response consists of four sub-surfaces. Each sub-surface represents a different failure mechanism. At the point where the material exceeds the failure surface, damage is initiated. The damage activation function F_N is introduced to describe the failure and damage evolution.

$$F_N = \phi_N - r_N \tag{3}$$

where ϕ_N is the function which depends on the stress state and the strength properties, r_N is the elastic domain thresholds, and N represents longitudinal ($N = 1+, 1-$) and transverse ($N = 2+, 2-$) directions. Initially r_N is 1 so that the material starts to be damaged when the function $F_N = 0$. The criterion for each microscopic failure mode is defined by the following equations.

For longitudinal (fibre) tensile and compressive failure,

$$\phi_{1+} = \frac{E_1}{X_T}\varepsilon_{11} = \frac{\tilde{\sigma}_{11} - \nu_{12}\tilde{\sigma}_{22}}{X_T} \tag{4}$$

$$\phi_{1-} = \frac{\langle|\tilde{\sigma}_{12}^m| + \eta^L \tilde{\sigma}_{22}^m\rangle}{S_L} \tag{5}$$

where ε is the stress tensor, $\tilde{\sigma}$ is the effective stress tensor, and X_T, S_L are the longitudinal tensile and the in-plane shear strength, respectively. η^L is the longitudinal friction coefficient and approximately defined as

$$\eta^L \approx -\frac{S_L \cos(2\alpha_0)}{Y_C \cos^2 \alpha_0} \tag{6}$$

where α_0 is the fracture angle in uniaxial compression, which is approximately 53°, $Y_C$is the transverse compressive strength. $\tilde{\sigma}^m$ is the effective stress tensor in a misalignment frame and derived from following equations.

$$\tilde{\sigma}_{22}^m = \tilde{\sigma}_{11}\sin^2\phi^c + \tilde{\sigma}_{22}\cos^2\phi^c - 2|\tilde{\sigma}_{12}| sin\phi^c cos\phi^c \tag{7}$$
$$\tilde{\sigma}_{12}^m = (\tilde{\sigma}_{22} - \tilde{\sigma}_{11}) sin\phi^c cos\phi^c + |\tilde{\sigma}_{12}|(\cos^2\phi^c - \sin^2\phi^c)$$

The parameter ϕ^c is the misalignment angle and kept constant during calculation.

$$\phi^C = \arctan\left(1 - \sqrt{\frac{1 - 4\left(\frac{S_L}{X_C} + \eta^L\right)\frac{S_L}{X_C}}{2\left(\frac{S_L}{X_C} + \eta^L\right)}}\right) \tag{8}$$

For transverse (matrix) failure: perpendicular to the laminate mid-plane,

$$\phi_{2+} = \begin{cases} \sqrt{(1-g)\frac{\tilde{\sigma}_{22}}{Y_T} + g\left(\frac{\tilde{\sigma}_{22}}{Y_T}\right)^2 + \left(\frac{\tilde{\sigma}_{22}}{S_L}\right)^2} & IF\ \tilde{\sigma}_{22} \geq 0 \\ \frac{\langle|\tilde{\sigma}_{12}| + \eta^L \tilde{\sigma}_{22}\rangle}{S_L} & IF\ \tilde{\sigma}_{22} < 0 \end{cases} \tag{9}$$

where g is the fracture toughness ratio of mode I to mode II.

For transverse (matrix) failure: transverse compression and shear,

$$\phi_{2-} = \sqrt{\left(\frac{\tilde{\tau}_{eff}^T}{S_T}\right)^2 + \left(\frac{\tilde{\tau}_{eff}^2}{S_L}\right)^2}\ \ IF\ \tilde{\sigma}_{22} < 0 \tag{10}$$

where the effective stress is derived as follows.

$$\tilde{\tau}_{eff}^T = \langle\tilde{\sigma}_{22}\, cos(\alpha_0)[sin(\alpha_0) - \eta^T\, cos(\alpha_0)\, cos\theta]\rangle \tag{11}$$
$$\tilde{\tau}_{eff}^L = \langle cos(\alpha_0)\,[|\tilde{\sigma}_{12}| + \eta^L \tilde{\sigma}_{22}\, cos(\alpha_0)\, sin\theta]\rangle$$

where θ is the sliding angle, S_T is the transverse shear strength, and η^T is the transverse friction coefficient defined as

$$\eta^T = \frac{-1}{tan(2\alpha_0)} \tag{12}$$

The damage variables $d_1, d_2,$ and d_6 are updated with the damage internal variable r_N after the stress state reaches the failure criterion. r_N is calculated for each failure mode, considering crack opening and closing events. In order for the damage evolution to account for objectivity, the dissipated energy is regularized as follows.

$$g_M = \frac{G_M}{l^*} \tag{13}$$

Where G_M is the fracture toughness, g_M is the dissipated energy per unit volume, and Mdenotes the failure mode ($M = 1+, 1-, 2+, 2-, 6$). l^* is the characteristic length of element which depends on the element size, element shape, and angle of the mesh lines with the crack direction.

3.2 Inter-lamina cohesive model

Delamination between inter-plies is modeled with an intrinsic cohesive zone approach implemented as MAT_138 of LS-DYNA in which the Bi-linear traction-separation law (TSL) is defined [14]. Fracture toughness in normal (mode I) and tangential direction (mode II) is defined as follows.

$$G_{Ic}^{int} = \frac{T\delta_I^F}{2} \tag{14}$$

$$G_{IIc}^{int} = \frac{S\delta_{II}^F}{2}$$

where T, S, δ_I^F, and δ_{II}^F are maximum stress and ultimate displacement in normal and tangential directions. Figure 4 shows a schematic representation of TSL in mixed mode. Mixed mode relative displacement is defined as

$$\delta_m = \sqrt{\delta_I^2 + \delta_{II}^2} \tag{15}$$

where $\delta_I = \delta_3$ is the separation in normal direction(mode I) and $\delta_{II} = \sqrt{\delta_1^2 + \delta_2^2}$ is the separation in tangential direction(model II). Once the mixed displacement fulfills the damage initiation criterion, stress starts to drop linearly from the peak stress to zero. The mixed mode damage initiation displacement δ^0 is defined as

$$\delta^0 = \delta_I^0 \delta_{II}^0 \sqrt{\frac{1+\beta^2}{(\delta_I^0)^2 + \beta(\delta_{II}^0)^2}} \tag{16}$$

where $\delta_{\mathrm{I}}^0 = T/EN$, $\delta_{\mathrm{II}}^0 = S/ET$. EN and ET represent initial stiffness in normal and tangential directions. After the damage is initiated, the irreversibility of the stress-displacement relation is considered with a single damage parameter until the displacement reaches the ultimate failure criterion. So if the material was unloaded after experiencing the damage initialization, the stress and strain would go back to the origin point. Displacement at the complete interface separation is defined as

$$\delta^F = \frac{2(2+\beta^2)}{\delta^0}\left[\left(\frac{EN}{G_{Ic}^{int}}\right)^2 + \left(\frac{ET \times \beta^2}{G_{IIc}^{int}}\right)^2\right]^{-\frac{1}{2}} \tag{17}$$

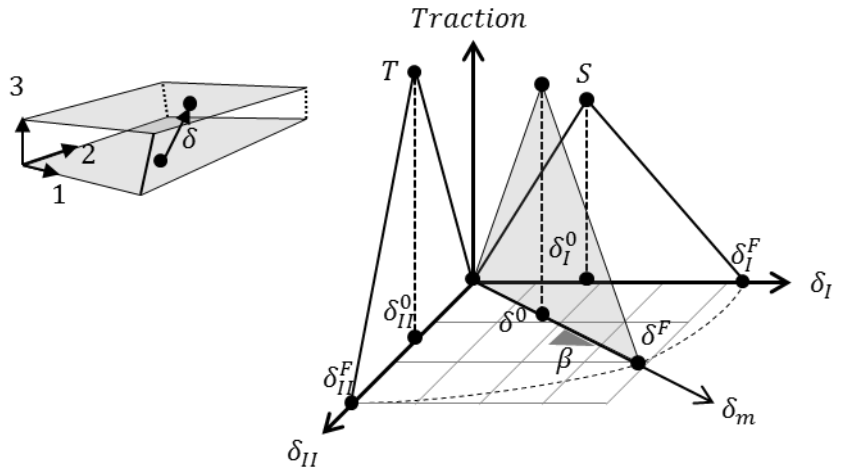

Figure 4: Mixed mode of bi-linear traction separation law. [14]

4 NUMERICAL SIMULATIONS

In this section, the axial crushing behaviour of a CFRP tube is analyzed with LS-DYNA. The geometry and material properties of the tube are referred to in the literature [8, 13] and the whole shape is modelled with 3D element technologies. Models which have different levels of mesh size and with and without a pre-defined debris model are analyzed, evaluating how the modelling affects the deformation mode and reaction force.

4.1 Simulation setup

A chamfered cylindrical CFRP tube from the reference [13] which is made from T700/QY8911 unidirectional prepreg tape is chosen and developed for LS-DYNA (Figure 5). The Lay-up is 14 plies of $[+45/-45/90/0/0/90/0]_s$ and each ply is modelled with 3D fully integrated shell elements with a size of about 1.0mm. The number of integration points through thickness in the element is 5. To consider delamination, cohesive elements are introduced between these ply layers, which share nodes of the connecting shells. Material properties are from the reference [8] except fracture toughness in fibre direction which is obtained from internal experiment and interfacial strength from the reference [13] (Table 1). These values are input parameters of MAT_262 for the inter-ply and MAT_138 for cohesive interface. A rigid platen is placed on top of the tube and moves down quasi-statically, considering contact with the tube. A friction coefficient of 0.4 applied between the platen and the structure. Bottom nodes of tube are fixed in all directions.

4.2 Element deletion

In crush analysis of composites with the finite element method, elements are deformed so much that the calculation stops due to numerical errors like negative Jacobian of shells or extremely large momentum of nodes. The damage model used in this study, in which stress starts to degrade and go down zero after damage initiation, is especially likely to suffer from this issue. Therefore a numerical technique for element deletion is mandatory in order for the simulation to be stable.

One approach is killing the integration point depending on its failure mode. For example, it can be assumed that the integration point failed and no more stress update is processed if it has fibre compressive or tensile failure, because in that case resistance left in the integration point is only in transverse direction, which is a relatively smaller strength. Element is deleted after all the integration points are failed. Another approach is leaving the element no matter what failure mode it has, but deleting the element only if it has negative Jacobian or its effective strain becomes large. In this approach, the integration point keeps being updated unless it causes a fatal error to the numerical algorithms. In this study, we tried these two methods to see how they affect the result.

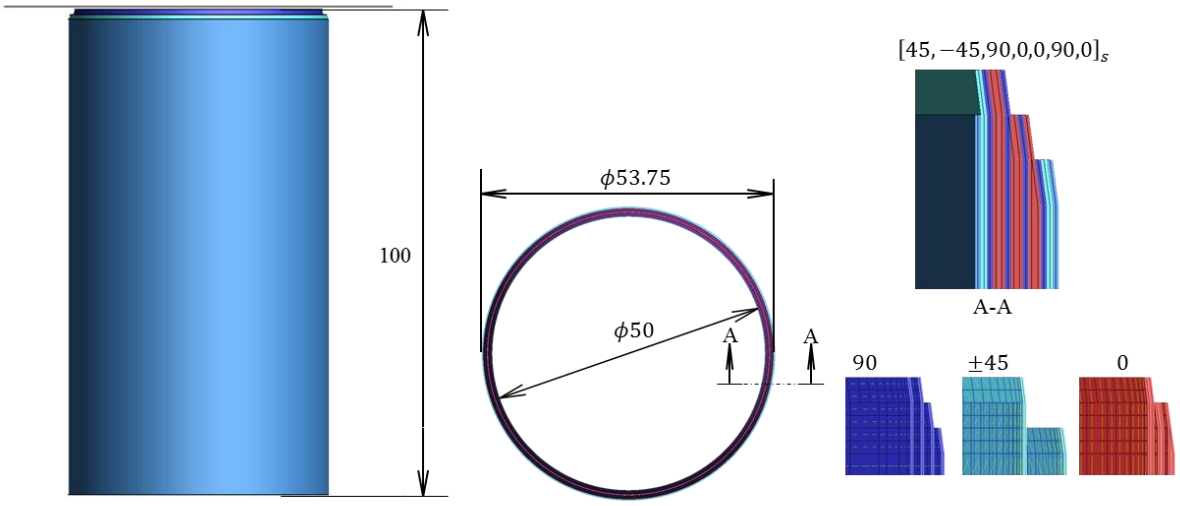

Figure 5: Axial crush simulation model.

Property	Symbol	Value
Modulus in fibre direction	E_1	1.35*GPa*
Modulus in transverse direction	E_2	9.12*GPa*
Poisson ratio	ν_{21}	0.021
In plane shear modulus	G_{12}	5.67*GPa*
Tensile strength in fibre direction	X_T	2326M*Pa*
Compressive strength in fibre direction	X_c	1236*MPa*
Tensile strength in transverse direction	Y_T	51*MPa*
Compressive strength in transverse direction	Y_c	209*MPa*
In-plane shear strength	S_L	87.9*MPa*
Tensile fracture toughness in fibre direction*	G_{XT}	182.13mJ/mm^2
Compressive fracture toughness in fibre direction*	G_{XC}	97.44 mJ/mm^2
Tensile fracture toughness in transverse direction	G_{YT}	0.425 mJ/mm^2
Compressive fracture toughness in transverse direction	G_{YC}	1.1mJ/mm^2
In-plane shear fracture toughness	G_{SL}	0.587mJ/mm^2
Interlaminar strength in normal direction**	T	99.2*MPa*
Interlaminar strength in tangential direction**	S	99.2*MPa*
Interlaminar fracture toughness in normal direction	G_{IC}^{int}	0.425mJ/mm^2
Interlaminar fracture toughness in tangential direction	G_{IIC}^{int}	0.587mJ/mm^2
Density	ρ	1.65ton/mm^3

* : obtained from internal experiment
** : reference [13]

Table 1: Material property data of chamfered cylindrical CFRP tube [8]

Figure 6 shows the stroke of the platen versus its reaction force, and Figure 7 shows a section cut in the crush front at the stroke 20mm. Large oscillation in reaction force can be seen in the case of failure mode based element deletion. For comparison, the filtered curve of the former case is plotted as well. This oscillation is caused by premature element deletion, which leads to loss of contacting material with the rigid platen. In the case of shape based element deletion, though initially the force oscillation is seen as well, it is gradually decreased after the stroke reaches 15mm. Since elements stay between the structure and platen and work as a debris wedge, the reaction force becomes stable and the elements induce successive damaging in the crush front. It is noticeable that the filtered curve of the

former case is obviously smaller than that of the latter case due to the lack of elements which supposed to transfer the load after a progressive failure mode is initiated.

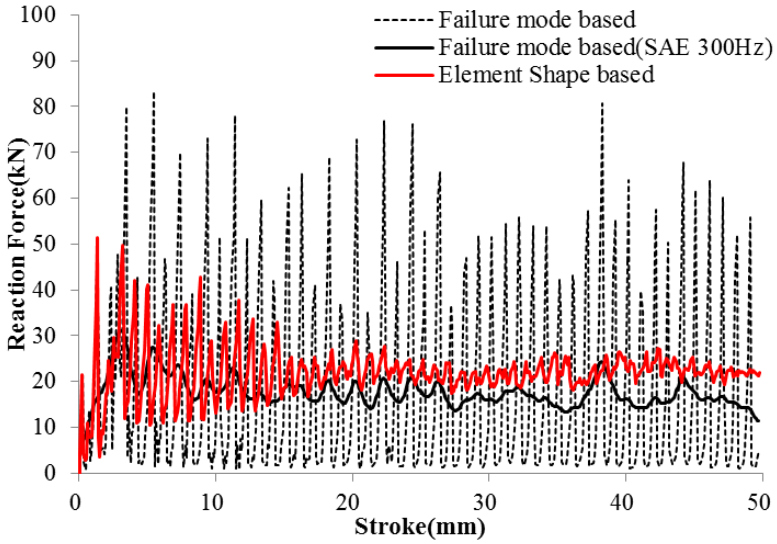

Figure 6: Comparison of reaction force of the different approaches of element deletion.

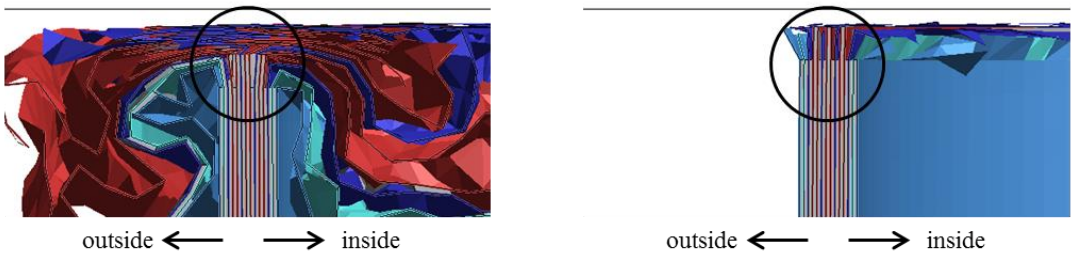

(a) : Element Shape based deletion (Crash Front)

(b) : Failure mode based deletion (Crash Front)

Figure 7: Comparison of deformation of the different element deletion approaches.

4.3 Influence of mesh size and crush front modelling

In this section, we describe the effect of the mesh size on the reaction force and deformation mode in the crush front with the shape based element deletion method mentioned in the previous section. Furthermore, numerical study with a pre-defined debris wedge is conducted in order to see how the shape of debris affects the result.

The same chamfered cylindrical tube model which has different element size, 0.5mm, is prepared and analyzed under compressive loading in the same way as the previous section. Figure 7 (a) shows the displacement of the platen versus its reaction force and (b) shows deformation of 0.5mm mesh model. The averaged reaction force after the stroke 15mm and the force level (maximum and minimum force after 10mm of the stroke) measured in the experiment [8] are also presented. Oscillation of the reaction force is observed in both cases of simulation but it is larger in the case of mesh size 1.0mm. In both cases, the oscillation gets smaller and the force keeps at a nearly constant level as deformation becomes stable by the stroke 15mm. However, it is noticeable that the force level of the 0.5mm mesh model is larger than that of the 1.0mm model by about 20 to 30%. Figure 8 shows the section cut of the crush front of both models at the strokes 4mm and 20mm. In the early stages of the crushing event, plies are subjected to compressive loading and have buckling and kinking deformation, which corresponds to beginning of the debris wedge formation. In this phase, the difference in reaction force levels between both cases is still small. As the deformation progresses, the

appearance of the debris wedge is different depending on the mesh size. In the cross sectional image, a more localized debris formation can be seen in the case of the smaller mesh size. The difference of the debris wedge formation is apparent at the stroke 20mm. At this time, the force level in smaller mesh size is around 20 to 25kN, whereas in the finer mesh it is 28 to 30kN which is very close to the experiment result [8].

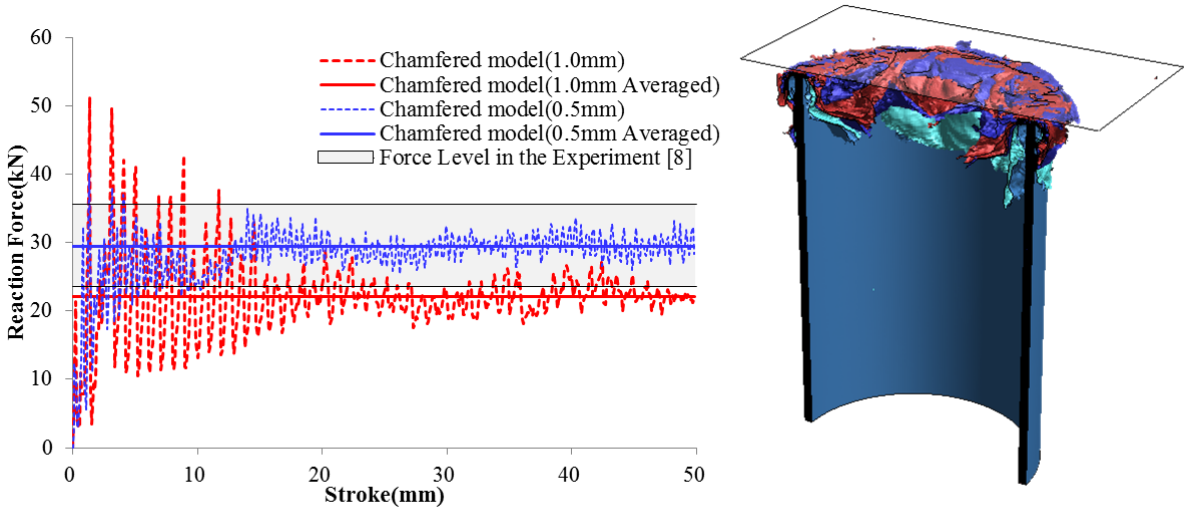

(a) Comparison of reaction force of the different mesh size (b) Deformation of 0.5mm mesh model

Figure 7: Force and displacement curves and deformation mode

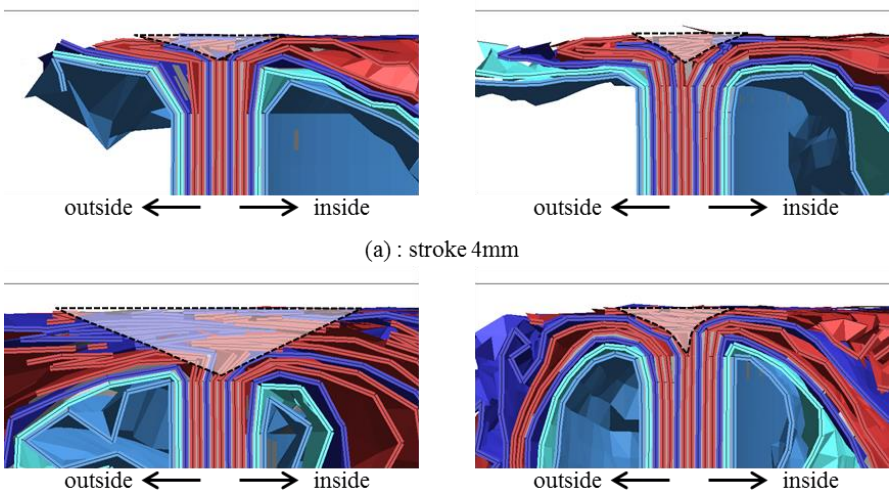

Figure 8: Comparison of deformation mode in crush front (left : 1mm mesh, right : 0.5mm mesh).

The method using a pre-defined debris wedge, which is initially placed on top of tube structure, is one of the effective techniques for evaluating the characteristics of a composite tube under axial crush loading [6, 7]. Based on the previous study of mesh size effect, two debris models (A and B, Figure 9) which have different sizes are prepared and attached to the platen. The same analysis is done with 0.5mm mesh and the artificial debris wedge. Figure 10 shows the displacement of the platen versus its reaction force and Figure 11 shows the cross sectional image in the crush front of two cases. There is a clear correlation between the size of debris wedge and reaction force. The smaller the size of debris

wedge, the higher reaction force that is observed. This trend corresponds to the study of mesh size dependency.

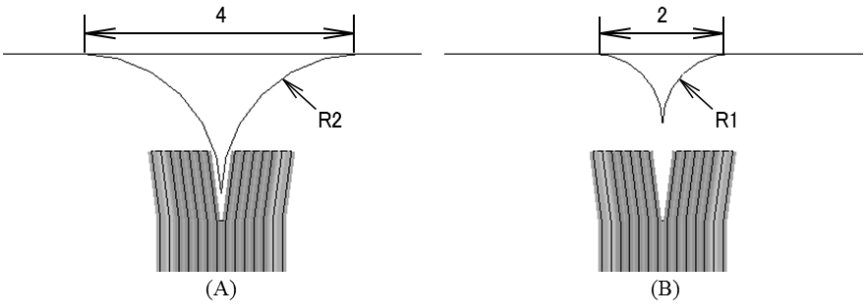

Figure 9: Pre-defined debris model which is different in size.

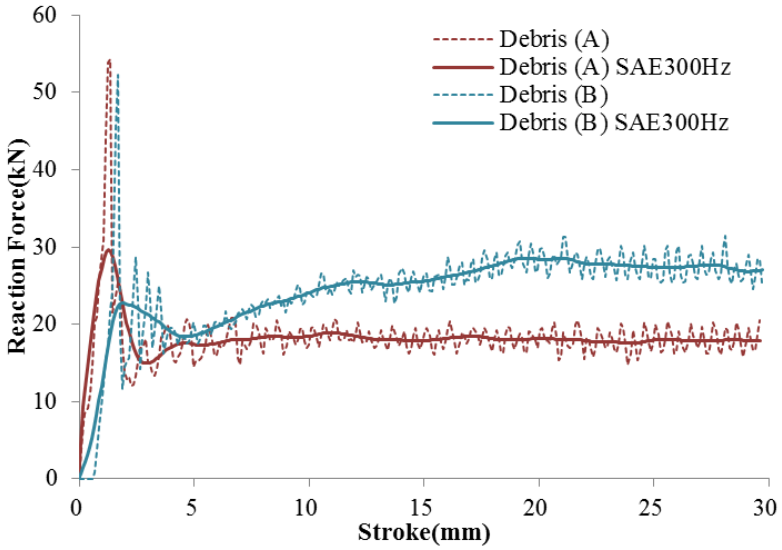

Figure 10: Comparison of reaction force of different debris size.

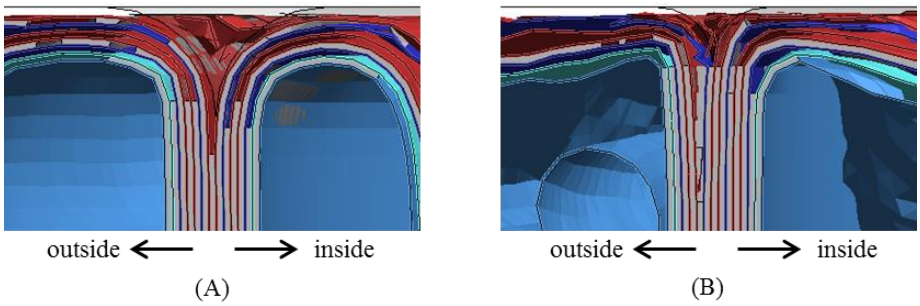

Figure 11: Comparison of deformation mode of different debris size in crush front.

4.3 Discussion

In the previous study, it is observed that the formation and the size of aggregates which consist of crushed composite materials have great effect on deformation mode and reaction force which are important for the evaluation of energy absorption of the composite structure. In the mesh size study, the formation of debris is expressed as a result of buckling of shell elements and contact processing

between these elements. Therefore, each model generates different shape and size of debris in the crush front of the composite tube. According to the study of the pre-defined debris model, it is observed that the deformation mode and reaction force strongly depend on the size of debris model. In the case of large size of debris in depth, the deformation mode of the ply sheet is bending dominant, whereas the case of smaller size of debris makes the ply sheet be subjected to compression dominant deformation until it reaches the platen. In the latter case, high compression strength of fiber direction can contribute largely to reaction force, which yields a relatively larger reaction force compared to the case of the larger debris model. Consequently, each case shows quite different capability of energy absorption, although the shape of the structure is completely the same.

From the observation above, reproducing how the debris is generated is a key issue for computational evaluation of composite structures which are subjected to compression loading. Higher prediction accuracy for the debris wedge formation is required. As is well known, the debris wedge is generated as a consequence of compression after material failure. In conjunction with the failure mode, robust element formulation and adequate modelling technique which can accept a large degree of discontinuity and reproduce the complex nature of material behavior is required in order to achieve an accurate simulation.

9 CONCLUSIONS

Axial crushing simulation of a CFRP tube was performed with an explicit finite element solver, LS-DYNA. Physically based material and failure models applied to composite ply, and cohesive elements are used to model the laminated tube structure. The numerical simulation, which can produce a bunch of discontinuity with a large deformation of the structure, needs numerical techniques like element deletion in order to achieve robust calculation. In this study, we evaluated two kinds of element deletion strategies and confirmed that the way in which failed elements becomes a debris wedge is appropriate for this kind of simulation. In the numerical simulation, elements which experienced certain failure modes can play an important role to transfer reaction force to the structures and induce successive failure in the crush front area, forming a debris wedge which is observed in the real composite failure, even though they no longer have the original strength. This contribution results in reproducing a more realistic response and deformation mode.

We also investigated the effect of element size to see how the difference appears in the result. A finer mesh model yielded more localized debris formation, while reaction force is higher compared to a larger mesh model. Furthermore, we investigated how the different debris size affects the result. The study showed that smaller debris causes compression dominant deformation rather than bending mode for the ply, which results in higher reaction force.

These two kinds of investigation are consistent with each other. It also implies that it is important for numerical simulation of the composite structure to predict the formation of the debris wedge. This is because the debris formation, which means not only the size, but also the location, can decide successive damage progression and deformation mode in the material which directly relate to the capability of energy absorption of the structure. However, it is still challenging to reproduce such phenomena in which a large amount of discontinuity is produced and the crushed material contributes to the whole behavior of the structure. Considering the complex nature of debris formation, not only a sophisticated failure model, but also effective element formulation and modelling technique should be proposed in order to achieve an accurate prediction.

REFERENCES

[1] D. Hull, A unified approach to progressive crushing of fibre-reinforced composite tubes, *Composites science and technology*, **40.4**, 1991, pp. 377-421 (doi: 10.1016/0266-3538(91)90031-J).

[2] H. Hamada, S. Ramakrishna, and H. Satoh, Crushing mechanism of carbon fibre/PEEK composite tubes, *Composites*, **26.11**, 1995, pp. 749-755 (doi: 10.1016/0010-4361(95)98195-Q).

[3] J. Lemaitre and R. Desmorat, *Engineering damage mechanics: ductile, creep, fatigue and brittle failures*, Springer Science & Business Media, 2005.

[4] P. Ladeveze, E. LeDantec, Damage modelling of the elementary ply for laminated composites, *Composites science and technology*, **43.3**, 1992, pp. 257-267 (doi: 10.1016/0266-3538(92)90097-M).

[5] P. Feraboli, et al., LS-DYNA MAT54 modeling of the axial crushing of a composite tape sinusoidal specimen, *Composites Part A: Applied Science and Manufacturing*, **42.11**, 2011, pp. 1809-1825 (doi: 10.1016/j.compositesa.2011.08.004).

[6] C. McGregor, R. Vaziri, X. Xiao, Finite element modelling of the progressive crushing of braided composite tubes under axial impact, *International Journal of Impact Engineering*, **37.6** , 2010, pp. 662-672 (doi: 10.1016/j.ijimpeng.2009.09.005).

[7] S.T. Pinho, P. P. Camanho, and M. F. De Moura, Numerical simulation of the crushing process of composite materials, *International journal of crashworthiness*, **9.3**, 2004, pp. 263-276 (doi: 10.1533/ijcr.2004.0287).

[8] L.N.S. Chiu, B. G. Falzon, B. Chen, W. Yana, Validation of a 3D damage model for predicting the response of composite structures under crushing loads, *Composite Structures*, **147**, 2016, pp. 65-73 (doi: 10.1016/j.compstruct.2016.03.028).

[9] S.T. Pinho, L. Iannucci, and P. Robinson, Physically-based failure models and criteria for laminated fibre-reinforced composites with emphasis on fibre kinking: Part I: Development, *Composites Part A: Applied Science and Manufacturing*, **37.1**, 2006, pp. 63-73 (doi: 10.1016/j.compositesa.2005.04.016).

[10] S.T. Pinho, L. Iannucci, and P. Robinson, Physically based failure models and criteria for laminated fibre-reinforced composites with emphasis on fibre kinking. Part II: FE implementation. *Composites Part A: Applied Science and Manufacturing*, **37.5**, 2006, pp. 766-777 (doi: 10.1016/j.compositesa.2005.06.008).

[11] P. Maimí, P.P. Camanho, J.A. Mayugo, C.G. Dávila, *A continuum damage model for composite laminates: Part I–Constitutive model*, *Mechanics of Materials*, **39.10**, 2007, pp. 897-908 (doi: 10.1016/j.mechmat.2007.03.005).

[12] P. Maimí, P.P. Camanho, J.A. Mayugo, C.G. Dávila, A continuum damage model for composite laminates: Part II–Computational implementation and validation, *Mechanics of Materials*, **39.10**, 2007, pp. 909-919 (doi: 10.1016/j.mechmat.2007.03.006).

[13] J. Huang, W. Xinwei, Numerical and experimental investigations on the axial crushing response of composite tubes, *Composite Structures*, **91**, 2009, pp. 222-228 (doi: 10.1016/j.compstruct.2009.05.006).

[14] LIVEREMORE SOFTWARE TECHNOLOGY CORPORATION (LSTC), *LS-DYNA KEYWORD USER'S MANUAL*, Vol. 2 (Material Models), 2016.